PNAS RESEARCH ARTICLE | NEUROSCIENCE

Molecular signaling predicts corticospinal axon growth state and muscle response plasticity induced by neuromodulation

Neela Zareen[a], Halley Yung[a], Walter Kaczetow[b], Aliya Glattstein[a], Ekaterina Mazalkova[a], Heather Alexander[a], Liang Chen[a], Lucas C. Parra[c], and John H. Martin[a,d,1]

Affiliations are included on p. 11.

Edited by Peter Strick, University of Pittsburgh Brain Institute, Pittsburgh, PA; received May 11, 2024; accepted September 24, 2024

Electrical motor cortex stimulation can produce corticospinal system plasticity and enhance motor function after injury. We investigate molecular mechanisms of structural and physiological plasticity following electrical neuromodulation, focusing on identifying molecular predictors, or biomarkers, for durable plasticity. We used two neuromodulation protocols, repetitive multipulse stimulation (rMPS) and patterned intermittent theta burst stimulation (iTBS), incorporating different stimulation durations and follow-up periods. We compared neuromodulation efficacy in promoting corticospinal tract (CST) sprouting, motor cortex muscle evoked potential (MEP) LTP-like plasticity, and their associated molecular underpinnings. Only iTBS produced CST sprouting after short-term neuromodulation (1 d of stimulation; 9-d survival for sprouting expression); both iTBS and rMPS produced sprouting with long-term (10-d) neuromodulation. Significant mTOR signaling activation and phosphatase and tensin homolog (PTEN) protein deactivation predicted axon growth across all neuromodulation conditions that produced significant sprouting. Both neuromodulation protocols, regardless of duration, were effective in producing MEP enhancement. However, persistent LTP-like enhancement of MEPs at 30 d was only produced by long-term iTBS. Statistical modeling suggests that Stat3 signaling is the key mediator of MEP enhancement. Cervical spinal cord injury (SCI) alone did not affect baseline molecular signaling. Whereas iTBS and rMPS after SCI produced strong mTOR activation and PTEN deactivation, only iTBS produced Stat3 activation. Our findings support differential molecular biomarkers for neuromodulation-dependent structural and physiological plasticity and show that motor cortex epidural neuromodulation produces molecular changes in neurons that support axonal growth after SCI. iTBS may be more suitable for repair after SCI because it promotes molecular signaling for both CST growth and MEP plasticity.

axon sprouting | LTP | motor cortex | spinal cord

Significance

Movements become impaired after stroke or spinal cord injury due to weakening of connections between the cortex and spinal circuits. Neuromodulation using electrical stimulation drives axon sprouting and strengthens corticospinal connections for repair. We use repetitive and patterned stimulation to investigate molecular mechanisms for structural and LTP-like plasticity and identify neuromodulation biomarkers for durable plasticity. mTOR signaling activation and PTEN deactivation are biomarkers for axon sprouting and Stat3 activation, for LTP-like plasticity induced by neuromodulation. Spinal injury did not affect sprouting signaling, whereas signaling for LTP-like plasticity was neuromodulation protocol-dependent. Our findings reveal differential molecular biomarkers for predicting structural and physiological plasticity after neuromodulation and show that neuromodulation activates growth-promoting signaling, similar to what was achieved by manipulating gene expression.

With the goal of reestablishing lost functional connections between the motor cortex and muscle after injury, it is well established that a variety of motor cortex neuromodulation approaches can be used to induce corticospinal motor system plasticity (1–5). Human studies have used performance and physiological outcome measures to assess plasticity. Muscle responses evoked by transcranial magnetic stimulation of the motor cortex (i.e., motor evoked potentials, MEPs) are a common target for neuromodulation efficacy, as they capture the capacity to modulate the strength of connections to motoneurons and muscles (6). Studies have leveraged neuromodulation to produce short-term MEP enhancement (1, 7–10). The potential for using neuromodulation for long-term modification of corticomotor connectivity, necessary for durable recovery, is not well explored. We have previously shown that motor cortex neuromodulation using electrical stimulation in animals can produce significant corticospinal tract (CST) axon sprouting during development and maturity and, in turn, improvement in motor function after injury (11–14).

Our prior studies leveraged activity-dependent processes to promote CST axon outgrowth, based upon the importance of such mechanisms in establishment of CST connections during development (15). Using repetitive multipulse stimulation (rMPS), we showed that 10 d of daily rMPS promotes CST sprouting (12). This repetitive stimulation protocol can reactivate developmentally down-regulated signaling pathways for axon growth in neurons, especially mammalian target of rapamycin (mTOR) (16). rMPS also deactivates phosphatase and tensin homolog (PTEN), a negative regulator of mTOR signaling. Genetic deletion of PTEN promotes CST axon outgrowth (17, 18). Intriguingly, these findings suggest that motor cortex neuromodulation can replicate features of the upregulation of axon growth mechanisms shown by genetic manipulation, pointing to previously unrecognized clinical benefits for motor cortex neuromodulation. Intermittent

Author contributions: N.Z., L.C.P., and J.H.M. designed research; N.Z., E.M., H.A., and L.C.P. performed research; N.Z., H.Y., W.K., A.G., E.M., H.A., L.C., and L.C.P. analyzed data; L.C.P. and W.K. contributed to design of the statistical model; and N.Z., L.C.P., and J.H.M. wrote the paper.

The authors declare no competing interest.

This article is a PNAS Direct Submission.

[1]To whom correspondence may be addressed. Email: jmartin@med.cuny.edu.

This article contains supporting information online at https://www.pnas.org/lookup/suppl/doi:10.1073/pnas.2408508121/-/DCSupplemental.

Published November 13, 2024.

theta burst stimulation (iTBS), a patterned motor cortex electrical stimulation protocol known to promote long-term potentiation (LTP) in the hippocampus, motor cortex, and other brain regions (19), also produces CST sprouting (8). Motor cortex neuromodulation thus meets an important need to repair key voluntary motor control circuits after injury in animal models. However, there remains a significant gap in the understanding of the molecular underpinnings of neuromodulation-driven plasticity and repair and how this knowledge can help shape development of therapeutic neuromodulation protocols.

In this study, we target the motor cortex with epidural electrical neuromodulation in rats to engage mechanisms for axon growth in CST neurons and promote physiological (MEP) plasticity. We investigate molecular mechanisms for structural and physiological plasticity from the perspective of identifying markers for neuromodulatory protocols capable of predicting durable plasticity after cervical contusion spinal cord injury (SCI). Our goals are to identify molecular markers of CST growth and MEP enhancement induced by neuromodulation and to determine whether those markers express after cervical SCI. We determine neuromodulation protocols (rMPS and iTBS, for different stimulation and survival periods) in which CST axon growth and MEP plasticity are or are not produced, together or separately. Among those conditions, we show that mTOR signaling activation and PTEN protein deactivation are key molecular biomarkers for neuromodulation-dependent CST sprouting and that signal transducer and activator of transcription3 (Stat3) gene activation is the key biomarker for MEP enhancement. Comparison of naive and cervical SCI cohorts shows that CST growth signaling is preserved after injury but that preservation of MEP plasticity signaling is dependent on the neuromodulation protocol. Our findings support differential molecular biomarkers for structural and functional plasticity in intact and spinal injured animals and suggest that motor cortex neuromodulation can be used to mirror genetic manipulation for functional repair.

Results

Experimental Design. We examined the differential effects of rMPS and iTBS on CST sprouting, enhancement of MEP recruitment, and underlying molecular signaling in naive rats. Separate animal cohorts were subjected to short-term (single session) or long-term (10 daily sessions) motor cortex neuromodulation protocols (Fig. 1 and *SI Appendix*, Table S1; short-term and long-term are abbreviated ST and LT in figures and tables). Note, the short-term CST groups, 1M10 and 1T10, received 1 d of stimulation, followed by survival of nine additional days without stimulation. Our prior studies show that this is sufficient time to allow for CST sprouting to be expressed (e.g., ref. 12). For both cohorts, experiments were terminated after completion of the period of neuromodulation and follow-up testing without neuromodulation for the purpose of studying the persistence of CST, MEP, and molecular changes. A separate cohort of rats was subjected to midline cervical (C4) SCI to determine the effects of neuromodulation on molecular signaling after CST axotomy.

iTBS and rMPS Enhance CST Sprouting, But Only iTBS Produces Sprouting with Short-Term Stimulation. We first determined the differential capacities for rMPS and iTBS to induce sprouting using short-term motor cortex neuromodulation, examined at 9 d after stimulation ended to provide adequate survival time for sprouting (12). *SI Appendix*, Fig. S1 shows the method used for CST axon length measurement. rMPS was not different from shams (Fig. 2*A*). Representative examples of CST labeling are shown in *SI Appendix*, Fig. S2. In contrast to rMPS, short-term iTBS produced significant CST sprouting compared with baseline (Fig. 2*A*, 1T10). For

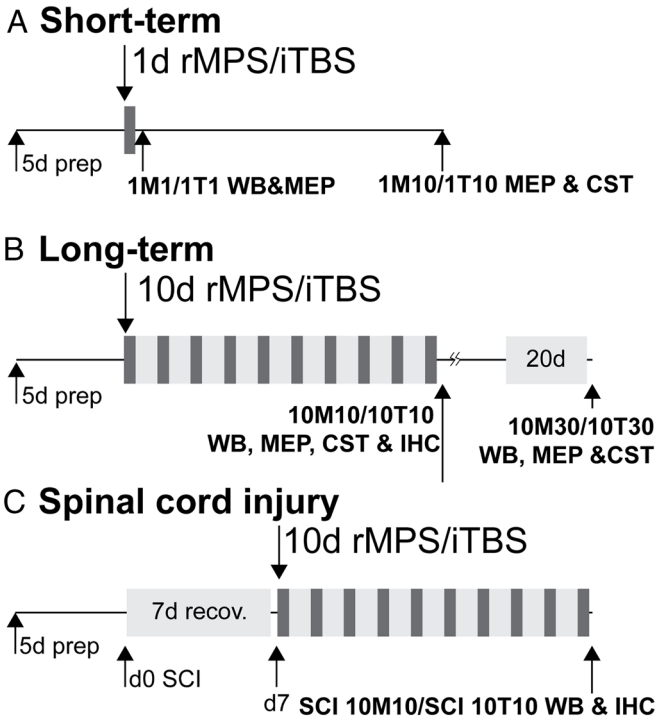

Fig. 1. Experimental timeline. Experimental timeline showing events of motor cortex stimulation and subsequent experiments and follow-up period. Dark gray bars represent daily stimulation. (*A*) Short-term stimulation groups: Subgroups are subjected to western blotting (WB), electrophysiology, or CST sprouting experiments. (*B*) For long-term stimulation groups, the rats either received 10 d of daily stimulation followed by MEP examination and termination of the experiment or followed by 20 additional days without stimulation. (*C*) Spinal cord injured group, which is subjected to WB only.

long-term neuromodulation, rMPS was transformed into a growth-promoting protocol when stimulation was applied daily for 10 consecutive days (Fig. 2*B*; 10M10). Long-term iTBS at 10-d survival (10T10) produced similar results as short-term iTBS. CST sprouting was maintained at the 30-d late follow-up with long-term rMPS and iTBS (Fig. 2*B*, 10M30; 10T30). These findings show differential axon growth potential for the two neuromodulation protocols and further show that neuromodulation duration is not the sole determinant of the capacity for CST axon growth and maintenance. These data form a basis for subsequent comparison with MEP enhancement and molecular signaling changes.

CST Axonal Sprouting Is Not a Determinant of Motor Cortex MEP Plasticity. We next determined the association between CST sprouting and MEP enhancement (see *SI Appendix*, Fig. S3 for sample MEP EMG raster plot). For short-term neuromodulation, MEP enhancement was assessed for each animal at baseline, the day after a single neuromodulation session (1M1 and 1T1), and 9 d later (1M10 and 1T10). Representative examples of MEPs recorded before and after short-term rMPS and iTBS show enhancement after neuromodulation and loss of enhancement when retested on day 10 (Fig. 3 *A* and *B*). Long-term rMPS, produced similar MEP enhancement when tested after cessation of neuromodulation on day 10, but when retested on day 30, responses returned to baseline (Fig. 3*C*). By contrast, MEPs are enhanced after long-term iTBS and this enhancement persists on day 30 (Fig. 3*D*).

We quantified these findings by constructing recruitment curves [area under the MEP response curve (AUC); Fig. 4]. For short-term stimulation, rMPS and iTBS both produced a significant increase in MEP recruitment slope and significant increases in individual MEP response measurements at 1.2 to 1.6 of threshold for ST rMPS and 1.3 to 1.6 of threshold for ST iTBS, the day after

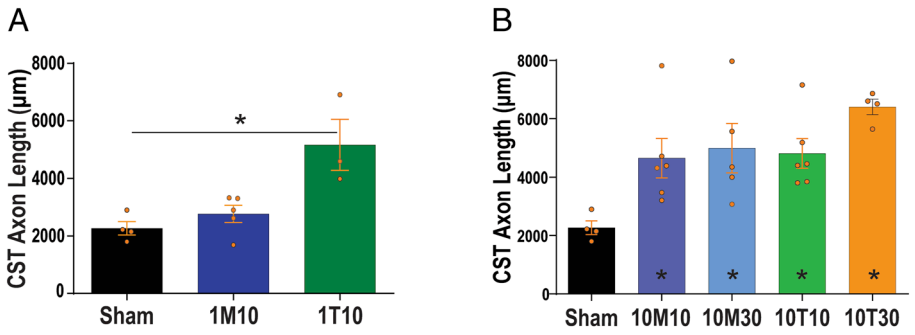

Fig. 2. CST sprouting after MPS and iTBS (see Fig. 1 for experimental group abbreviations). (*A*) Quantification of CST sprouting contralateral CST axons following short-term stimulation. The asterisk denotes significant differences from the sham. *P = 0.033 (Control vs. 1T10); One-way ANOVA with Dunnett's multiple comparisons test. Sham, n = 4; 1M10, n = 5; 1T10, n = 3. (*B*) As *A* but following long-term stimulation. Asterisks denote significant differences from the sham. Post hoc tests revealed the following: *P = 0.039 (sham vs. 10M10); *P = 0.0204 (sham vs. 10M30); *P = 0.0257 (sham vs. 10T10); *P = 0.0007 (sham vs. 10T30). One-way ANOVA with Dunnett's multiple comparisons test. Sham, n = 4; 10M10, n = 6; 10M30, n = 5; 10T10, n = 6 and 10T30, n = 4.

neuromodulation. However, recruitment slope returned to baseline on day 10 for both stimulation protocols (Fig. 4 *A* and *B*).

For long-term neuromodulation, we tested MEP recruitment at baseline, after 10 d of neuromodulation (nominally delayed for threshold and response stability; see *Materials and Method*), and on day 30. For rMPS, individual MEP responses were significantly greater at 1.3 to 1.6 of threshold and the recruitment slope was significantly increased after neuromodulation but returned to baseline on day 30 (Fig. 4*C*). Despite significant CST sprouting at the 30-d time point (Fig. 2), there was no MEP enhancement at this time point. For iTBS, MEP recruitment measurements show significant increases at 1.5 and 1.6 of threshold and increased recruitment slope at the 10-d follow-up (10T10). Importantly, at 30-d follow-up MEP values and recruitment slope remained significantly increased (Fig. 4*D*). Long-term iTBS produced CST sprouting at both time points (Fig. 2). These findings show remarkable persistence of MEP enhancement after iTBS and that CST sprouting is neither necessary nor sufficient for MEP enhancement.

Neuromodulation Produces Distinctive Molecular Changes. To understand differential molecular mechanisms underlying CST sprouting and MEP enhancement in animals receiving rMPS versus iTBS, we performed western blotting (WB) for mTOR, PTEN, and Jak/Stat signaling after short- and long-term treatments. mTOR signaling was assayed by the ratio of the levels of the ribosomal protein S6 phosphorylated at S235/S236 residues (pS6), which indicates active mTOR signaling (20, 21), and total

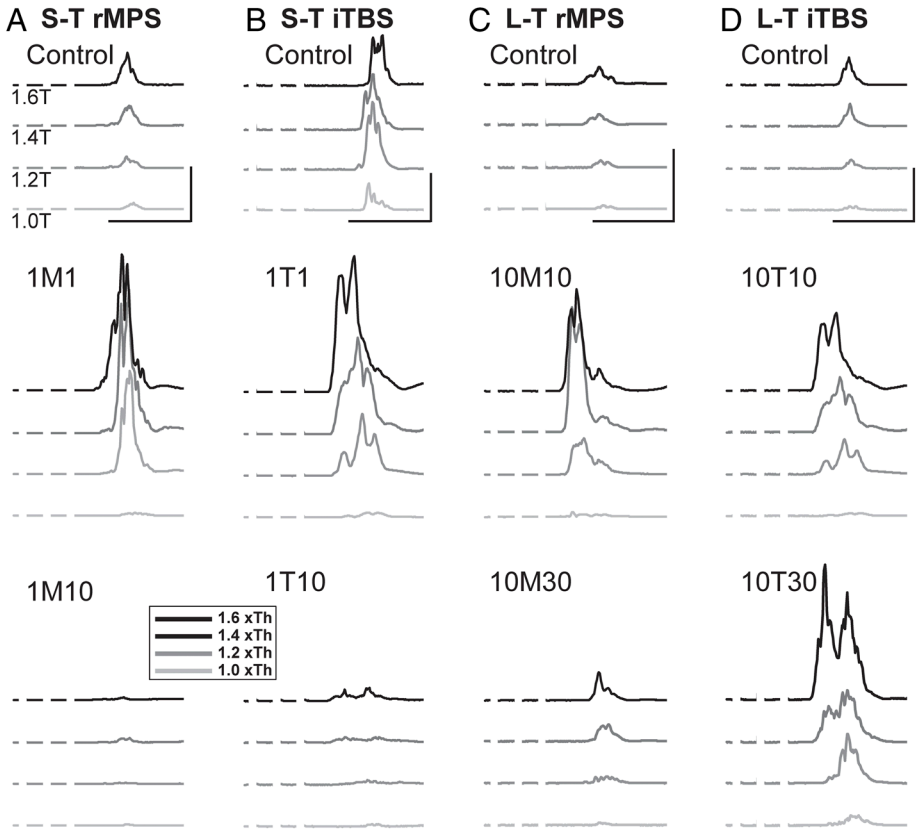

Fig. 3. MEP enhancement after short-term and long-term motor cortex neuromodulation. Average MEP tracings of all frames delivered (n = 20) from electrophysiological experiments conducted in four representative animals (conditions indicated for each) at threshold (1.0), 1.2 T, 1.4 T, and 1.6 T (indicated for part A, control; light gray to black). The three short gaps in the beginning of the recordings correspond to the stimulus artifacts, which have been blanked. Calibrations: Time: *A*–*D*, 10 ms; amplitude: *A*, 125 µV; *B*, 145 µV; *C*, 100 µV; *D*, 128 µV.

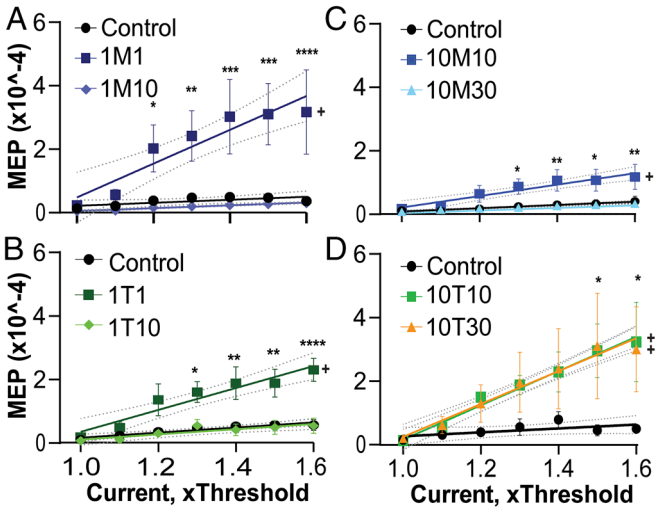

Fig. 4. Enhancement of MEP recruitment after short-term and long-term motor cortex neuromodulation. MEP responses were quantified by measurement of the AUC of the averaged rectified ECR muscle response. (*A*) Short-term MPS. Control data consist of MEPs that were recorded before rMPS, 24 h after rMPS (1M1), and 9 d after rMPS (1M10). Linear regression line (solid) and CI (broken lines) are shown. Plus (+) signs show significant differences in slope of linear regression lines calculated via one-way ANOVA with Tukey's multiple comparison test. ^{+}P = 0.0001 for slopes of MEP enhancement at control vs. 1M1 and for 1M1 vs. 1M10. Slopes of control vs. 1M10 were not significantly different; P = 1.0. Asterisks represent significant differences in the AUC measured at each input current (i.e., 1.2× the threshold current, which is abbreviated as 1.2 and 1.0, respectively), determined using two-way ANOVA with Tukey's multiple comparison test. ****P < 0.0001 (Control vs. 1M1 at 1.6 T); ***P = 0.0004 (Control vs. 1M1 at 1.5 T and 1.4 T); **P = 0.0096 (Control vs. 1M1 at 1.3 T); and *P = 0.0376 (Control vs. 1M1 at 1.2 T). N = 3. (*B*) As for part *A*, but for short-term iTBS. ^{+}P = 0.001 for slopes of MEP enhancement at control vs. 1T2; and ^{+}P = 0.0032 for 1T1 vs. 1T10. The slopes of control vs. 1T10 were not significantly different; P = 1.0. Two-way ANOVA of AUC comparisons: ****P < 0.0001 (Control vs. 1T1 at 1.6 T); **P = 0.0053 (Control vs. 1T1 at 1.5 T); **P = 0.0035 (Control vs. 1T1 at 1.4 T); *P = 0.026 (Control vs. 1T1 at 1.3 T). Significant differences were observed between 1T1 vs. 1T10 at 1.6 T, 1.5 T, and 1.4 T. ***P = 0.002, **P = 0.006, and **P = 0.0034, respectively. N = 4. (*C*) As above, but MEP enhancement in response to long-term MPS. MEP responses were recorded before motor cortex neuromodulation, 3 d after (10M10 and 10T10), and 30 d after neuromodulation started (10M30 and 10T30). ^{+}P = 0.01 for Slopes of MEP enhancement at control vs. 10M10 and ^{+}P = 0.0093 for 10M10 vs. 10M30. Slopes of control vs. 10M30 were not significantly different; P = 0.97. Black asterisks represent significant differences in the AUC measured for each input current, determined using two-way ANOVA with Tukey's multiple comparison test. **P = 0.0073 (Control vs. 10M10 at 1.6 T); *P = 0.0106 (Control vs. 10M10 at 1.5 T); **P = 0.008 (Control vs. 10M10 1.4 T); *P = 0.0355 (Control vs. 10M10 at 1.3 T). Similar significant differences were observed between 10M10 vs. 10M30 at 1.6 T, 1.5 T, 1.4 T, and 1.3 T: **P < 0.0001, ****P = 0.0054, *P = 0.011, **P = 0.0081, and *P = 0.034, respectively. N = 5. (*D*) As part *C*, but for long-term iTBS. ^{+}P = 0.0076 for slopes of MEP enhancement at control vs. 10T10; and ^{+}P = 0.0202 for Control vs. 10T30. Slopes of 10T10 and 10T30 were not significantly different; P = 0.99. Two-way ANOVA of AUC comparisons: *P = 0.0138 (Control vs. 10T10 at 1.6 T); *P = 0.0258 (Control vs. 10T10 at 1.5 T). Significant differences were observed between Control vs. 10T30 at 1.6 T and 1.5 T; *P = 0.0399 and *P = 0.0273, respectively. N = 4.

S6. To determine changes in PTEN signaling, we examined the ratio of the levels of PTEN phosphorylated at the S380 residue (pPTEN), which is an inactive form of PTEN (22, 23), and total PTEN. For Jak/Stat, we measured the ratio of the levels of Stat3 phosphorylated at the Y705 residue, indicating active Jak/Stat signaling [pStat3; (24)], and total Stat3.

We first examined protein expression changes after short-term neuromodulation. For pS6 (Fig. 5*A*), representative western blots (A1) and quantification (A2) show a strong and significant increase after neuromodulation ends (1M1) but a return to baseline by day 10 (1M10), the follow-up period used for CST sprouting assessment. By contrast, iTBS shows increased levels after neuromodulation ends (1T1) and maintenance at day 10 (1T10). There was no change in total S6 for either protocol (Fig. 5, *A*3). For pPTEN (Fig. 5*B*), there were no significant changes with short-term rMPS (Fig. 5, *B*1 and *B*2). By contrast, for short-term iTBS there was a significant elevation in pPTEN levels on day 1 (i.e., PTEN deactivation), with maintenance of a significant elevation at day 10. For both protocols, there were no changes in total PTEN (Fig. 5, *B*3). Finally, ST-rMPS and ST-iTBS both produced the same pattern of pStat3 changes (Fig. 5*C*): significant elevation following 1 d of neuromodulation and not significantly different from baseline at 10 d (Fig. 5, *C*1 and *C*2). There was no change in total Stat3 (Fig. 5, *C*3).

For long-term neuromodulation (Fig. 6 *A*–*C*), we replicated earlier western blot findings for rMPS at a 10-d survival (16) for within-study comparison with iTBS and for testing long-term persistence of both protocols at day 30. For both pS6 and pPTEN (Fig. 6 *A* and *B*), there were strong and significant elevations at 10 d and 30 d (10M10, 10M30; 10T10, 10T30) for both rMPS and iTBS (Fig. 6, *A*1, *A*2, *B*1, and *B*2). For pStat3 (Fig. 6*C*), although protein levels are elevated at day 10 for both stimulation protocols, at the 30-d time point, the values are not different from baseline after rMPS but significantly elevated for iTBS (Fig. 6, *C*1 and *C*2). Total protein levels were not changed for pS6 (*A*3), pPTEN (*B*3), or pStat3 (*C*3). These findings provide support for distinctive effects of neuromodulation for all three molecules and raise an intriguing dissociation between Jak/Stat signaling with that of mTOR and PTEN, which is addressed next.

Molecular Markers of CST Axon Growth and MEP Enhancement. We next examined the protein expression patterns associated with CST sprouting and MEP plasticity to determine predictive molecular markers for the capacity of different neuromodulation protocols to produce CST sprouting and MEP enhancement. The western blot analyses reveal the pattern of changes in pS6, pPTEN, and pStat3 levels (i.e., mTOR, PTEN, and Jak/Stat signaling changes, respectively) across the different stimulation conditions (summarized in Fig. 7*A*). iTBS produced significant CST axonal sprouting and significant enhancement of pS6 and pPTEN for all conditions tested. rMPS produced CST sprouting for all but the short-term protocol (1M10), where neither pS6 nor pPTEN were elevated. Individual animal results reveal a strong correlation between pS6 and pPTEN across all conditions tested (R^2 = 0.45; P < 0.0001; n = 37; Fig. 7*B*). Data points from groups that showed significant CST sprouting are localized within the upper right quadrant of the plot, showing elevated protein levels (Fig. 7*B*; highlighted in red). All animals from these groups are enclosed in this region of the plot; excluded are animals from the neuromodulation group not showing significant outgrowth (1M10) and they clustered with sham animals (lower left quadrant). pS6 and pPTEN are both predictors of CST growth, and the underlying molecular changes reveal absolute threshold values for pS6 (0.786) and for pPTEN (0.64; dotted lines in Fig. 7*B*). The strong association between pS6 and pPTEN expression and CST outgrowth is illustrated graphically (Fig. 7*C*), where protein levels are rank-ordered according to their expression values and color coded according to whether or not each animal was part of a group that showed significant CST sprouting (blue) or not (gray).

Whereas pStat3 was elevated for many CST growth conditions, it was not elevated after 1T10 and 10M30, which are two conditions producing significant CST sprouting with iTBS and rMPS, respectively (Fig. 7*A*). Rank ordering of pStat3 protein levels (Fig. 7*C*) shows the lack of a threshold predicting growth, as we showed for pS6 and pPTEN. However, logistic regression revealed a statistically significant association between pStat3 protein levels and whether an animal was in a group that showed CST sprouting

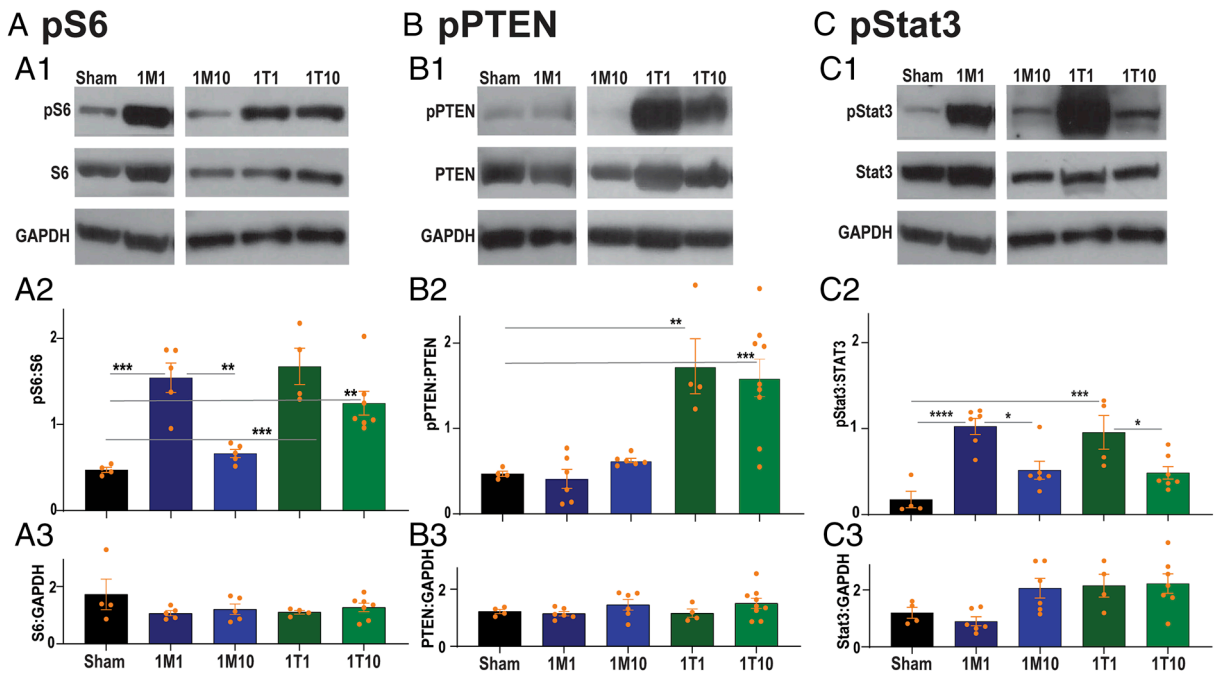

Fig. 5. Protein expression after short-term neuromodulation. (*A*) pS6 protein expression. (*A1*) Western blot images of cortical lysates probed with antisera against phospho-S6, total S6, and GAPDH. (*A2*) Mean intensities of pS6 expression, following short-term stimulation, presented as ratios of pS6 to total S6. Asterisks denote significant difference ***P = 0.0005 (Sham vs. 1M1); ***P = 0.0003 (Sham vs. 1T1); **P = 0.007 (Sham vs. 1T10); **P = 0.0023 (1M1 vs. 1M10). One-way ANOVA with Tukey's multiple comparisons test. Sham, n = 4; 1M1, n = 5; 1M10, n = 5; 1T1 = 4; 1T10, n = 7. (*A3*) Mean intensities of total S6 expression, presented as ratios of total S6 to GAPDH. One-way ANOVA with Tukey's multiple comparisons test shows no significant difference between groups. (*B*) pPTEN protein expression. (*B1*) Western blots probed with antisera against phospho-PTEN, total PTEN, and GAPDH. (*B2*) Mean intensities of pPTEN expression, following short-term stimulation, presented as ratios of pPTEN to total PTEN. Asterisks denote significant difference **P = 0.0064 (Sham vs. 1T10); ***P = 0.0005 (Sham vs. 1T10). Sham, n = 4; 1M1, n = 6; 1M10, n = 6; 1T1 = 4; 1T10, n = 9. (*B3*) Mean intensities of total PTEN expression, presented as ratios of total PTEN to GAPDH. One-way ANOVA with Tukey's multiple comparisons test shows no significant difference between groups. (*C*) pStat3 protein expression. (*C1*) Western blot probed with antisera against phospho-Stat3, total Stat3, and GAPDH. (*C2*) Mean intensities of pStat3 expression, following short-term stimulation, presented as ratios of pStat3 to total Stat3. Asterisks denote significant difference ***P = 0.0003 (Sham vs. 1M1); **P = 0.0019 (Sham vs. 1T1); *P = 0.0151 (1M1 vs. 1M10); *P = 0.047 (1T1 vs. 1T10). One-way ANOVA with Tukey's multiple comparisons test. Sham, n = 4; 1M1, n = 6; 1M10, n = 6; 1T1, n = 4; 1T10, n = 7. (*C3*) Mean intensities of total Stat3 expression, presented as ratios of total Stat3 to GAPDH. One-way ANOVA with Tukey's multiple comparisons test shows no significant difference between groups.

[t(35) = 2.698, P = 0.007, logistic model]. To summarize, iTBS and expression of pPTEN and pS6 were individual predictors of CST sprouting. As such, we cannot uniquely attribute their contribution, as we will do next for the MEP outcomes in a mediation analysis. The absence of pStat3 elevation after 1T10 suggests a neuromodulation protocol dependence.

For MEP plasticity, modulation of molecular signaling has a distinctive pattern from that of CST sprouting (Fig. 7*A*). Neither rMPS nor iTBS produced MEP plasticity for all stimulation conditions. rMPS did not produce MEP enhancement for the 1M10 and 10M30 conditions; iTBS did not produce MEP enhancement for the 1T10 condition. These dissociations revealed that neuromodulation protocols producing significant MEP enhancement also produce significant increases in pStat3 levels (Fig. 7*A*). When pStat3 is at baseline after neuromodulation, there is no MEP enhancement, and when significantly elevated, there is significant MEP enhancement. By contrast, the association between MEP plasticity and pS6 and pPTEN is inconsistent, both for short- and long-term conditions.

Rank-ordered protein values show the range over which MEP plasticity occurred for individual animals across the different groups (Fig. 7*D*; red bars, MEP plasticity animal groups; gray bars, no MEP plasticity). There were no absolute thresholds for any of the molecules for predicting MEP enhancement. We performed a mediation analysis to determine the effect of rMPS and TBS on MEP either directly or mediated by the three proteins (pPTEN, pStat3, and pS6; Fig. 7*E*). For the purpose of the model, we treated the three predictor proteins as independent measures. We recognize that, at least for pS6 and pPTEN, there may be interactions (e.g., PTEN is an upstream regulator of mTOR; see *Discussion*). The effect of pStat3 on MEP plasticity was significant [t(40) = 7.39, P = 0.0094] and trending for pS6 [t(40) = 3.04, P = 0.066], but the effect of pPTEN on MEP was not significant [t(40) = −1.32, P = 0.187; Fig. 7 *E*, *Right* side straight solid lines; *SI Appendix, Supplemental material 1* presents Matlab code; *SI Appendix, Supplemental material 2* presents model results]. Importantly, there was no evidence for a direct effect of either rMPS or iTBS on MEP (P = 0.80 and P = 0.28; Fig. 7*E*, dotted curved lines), indicating that neuromodulation drive of MEP plasticity is entirely through the molecular mediators. In contrast, all three protein markers were significantly affected by rMPS and iTBS (Fig. 7 *E*, *Left* side straight solid lines; *SI Appendix, Supplemental material*). The coefficients of the model suggest that the odds of observing MEP plasticity increase by a factor of 142 with the application of rMPS and by a factor of 107 with iTBS. For both types of stimulation, the odds of observing MEP enhancement are dominated by the mediation through pStat3 (*SI Appendix*, Table S2). Together this suggests that pStat3 is the dominant mediator of the neuromodulation on MEP with either stimulation protocol, with a possible smaller role for pS6, while pPTEN likely plays no role.

Neuromodulation Growth and Plasticity Biomarkers after Bilateral Cervical Contusion Are Similar to Naive Animals. Growth- and plasticity-promoting motor cortex neuromodulation protocols are most relevant for strengthening CS system connections after injury to promote recovery of motor function. We next determined whether the expected signaling changes with

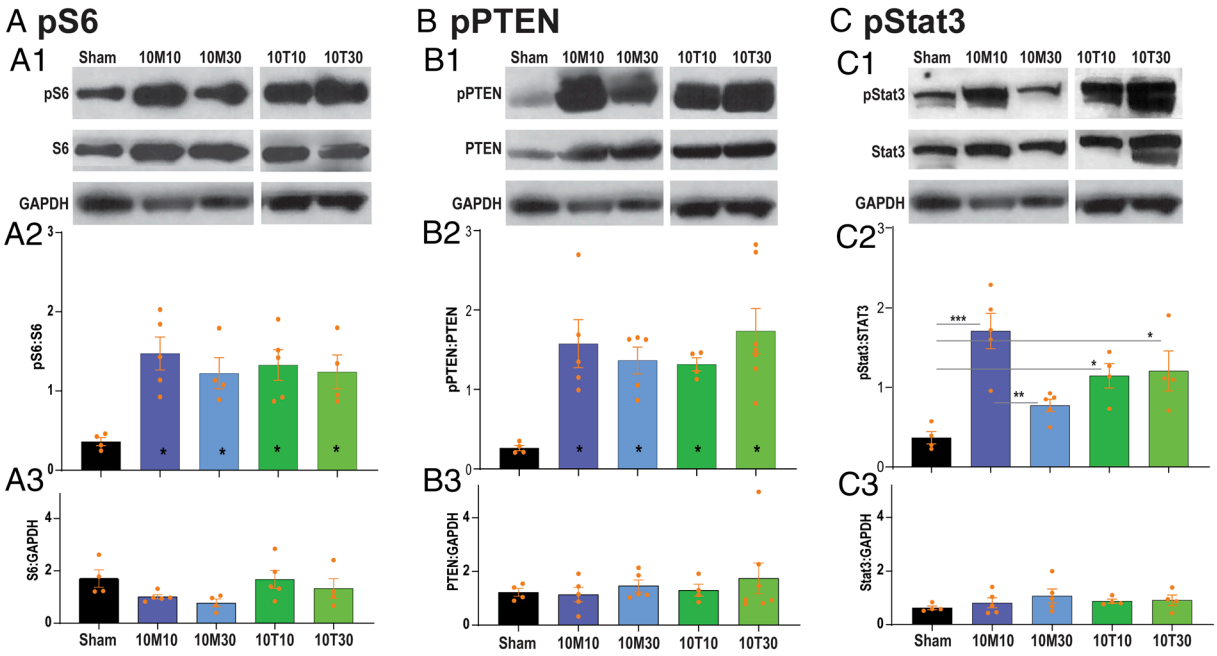

Fig. 6. Protein expression after long-term neuromodulation. (*A*) pS6 protein expression. (*A1*) Western blot images of cortical lysates probed with antisera against phospho-S6, total S6, and GAPDH. (*A2*) Mean intensities of pS6 expression, following long-term stimulation, presented as ratios of pS6 to total S6. Asterisks denote significant difference $^{**}P = 0.0048$ (Sham vs. 10M10); $^{*}P = 0.0456$ (Sham vs. 10M30); $^{*}P = 0.0149$ (Sham vs. 10T10); $^{*}P = 0.0404$ (Sham vs. 10T30). One-way ANOVA with Tukey's multiple comparisons test. Sham, n = 4; 10M10, n = 5; 10M30, n = 4; 10T10, n = 5; 10T30, n = 4. (*A3*) Mean intensities of total S6 expression, presented as ratios of total S6 to GAPDH. One-way ANOVA with Tukey's multiple comparisons test shows no significant difference between groups. (*B*) pPTEN protein expression. (*B1*) Western blot images of cortical lysates probed with antisera against phospho-PTEN, total PTEN, and GAPDH. (*B2*) Mean intensities of pPTEN expression, following long-term stimulation, presented as ratios of pPTEN to total PTEN. Asterisks denote significant difference $^{**}P = 0.0136$ (Sham vs. 10M10); $^{*}P = 0.0465$ (Sham vs. 10M30). $^{*}P = 0.0423$ (Sham vs. 10T10); $^{**}P = 0.0027$ (Sham vs. 10T30). Sham, n = 4; 10M10, n = 5; 10M30, n = 5; 10T10, n = 4; 10T30, n = 7. (*B3*) Mean intensities of total PTEN expression, presented as ratios of total PTEN to GAPDH. One-way ANOVA with Tukey's multiple comparisons test shows no significant difference between groups. (*C*) pStat3 protein expression. (*C1*) Western blot images of cortical lysates probed with antisera against phospho-Stat3, total Stat3, and GAPDH. (*C2*) Mean intensities of pStat3 expression, following long-term stimulation, presented as ratios of pStat3 to total Stat3. Asterisks denote significant difference $^{***}P = 0.0003$ (Sham vs. 10M10); $^{*}P = 0.0489$ (Sham vs. 10T10); $^{*}P = 0.0151$ (Sham vs. 10T30); $^{**}P = 0.0058$ (10M10 vs. 10M30). One-way ANOVA with Tukey's multiple comparisons test. Control group, n = 4; 10M10, n = 5; 10M30, n = 5; 10T10, n = 4; 10T30, n = 4. (*C3*) Mean intensities of total Stat3 expression, presented as ratios of total Stat3 to GAPDH. One-way ANOVA with Tukey's multiple comparisons test shows no significant difference between groups.

rMPS and iTBS in naive animals also occurred after a midline cervical contusion (*SI Appendix*, Fig. S5), which axotomizes the main (dorsal) CST in this injury model (14). For this experiment, we used 10M10 and 10T10, and evaluated molecular changes after the end of the final neuromodulation session. Cervical contusion SCI did not change baseline pS6, pPTEN, or pStat3 values, as shown in the representative western blots and associated quantification (Fig. 8 *A*–*C*; sham versus SCI). After injury, rMPS and iTBS both produced significant pS6 and pPTEN increases (SCI 10M10; SCI 10T10), similar to naive rats. By contrast, only iTBS produced a significant increase in pStat3 (Fig. 8, *C*1 and *C*2). These findings suggest that motor cortex neuromodulation up-regulates mTOR and down-regulates PTEN activity, both key components of CST growth signaling. Furthermore, since only iTBS additionally up-regulated pStat3, only this protocol could recruit both CST growth and MEP plasticity after SCI.

Discussion

Motor cortex neuromodulation leverages activity-dependent processes to enhance motor-cortex-to-muscle connections, to promote motor function and repair after injury (13, 14, 25, 26). Whereas most studies are agnostic to the extent to which neuromodulation targets structural or physiological plasticity, this is one of our study's prime objectives. Using two different motor cortex neuromodulation protocols (repetitive rMPS and patterned iTBS), together with different stimulation and follow-up durations, we determined the molecular signaling underpinning neuromodulation drive of CST axon sprouting and MEP enhancement. For CST growth signaling, we found that the presence of significant activation of mTOR signaling (pS6) and deactivation of PTEN protein (pPTEN) predicted axon growth across all neuromodulation conditions that produced significant CST sprouting. Although Jak/Stat signaling (pStat3) was not enhanced for some conditions, logistic regression revealed that it was significantly associated with CST growth protocols. For MEP enhancement, mediation analysis revealed that Jak/Stat (Stat3) signaling played a greater role than mTOR, with little or no role for PTEN. Our findings support distinct molecular predictors, or biomarkers, for structural and physiological plasticity. In doing so, our animal study sets efficacy expectations for developing neuromodulation to achieve structural and physiological plasticity of the corticospinal motor system.

Differential Neuromodulation Strategies for Promoting Structural and Functional Plasticity. mTOR activation, combined with PTEN protein deactivation, is central to the CST neuromodulation growth program. Our earlier study shows mTOR activation in motor cortex neurons after neuromodulation (16). Further, neuromodulation also up-regulates Stat3 neuronal and non-neuronal signaling (*SI Appendix*, Fig. S4). Intriguingly, there also is upregulation of mTOR and Stat3 signaling in non-neuronal cells, presumably glia, in the motor cortex after neuromodulation (16) (*SI Appendix*, Fig. S4). This was examined using immunohistochemistry for Survivin, a transcriptional target for Stat3 signaling (*SI Appendix*, Fig. S4). Comparison across the four treatment groups revealed differential protein activation patterns with rMPS and iTBS. Short-term rMPS failed to phosphorylate

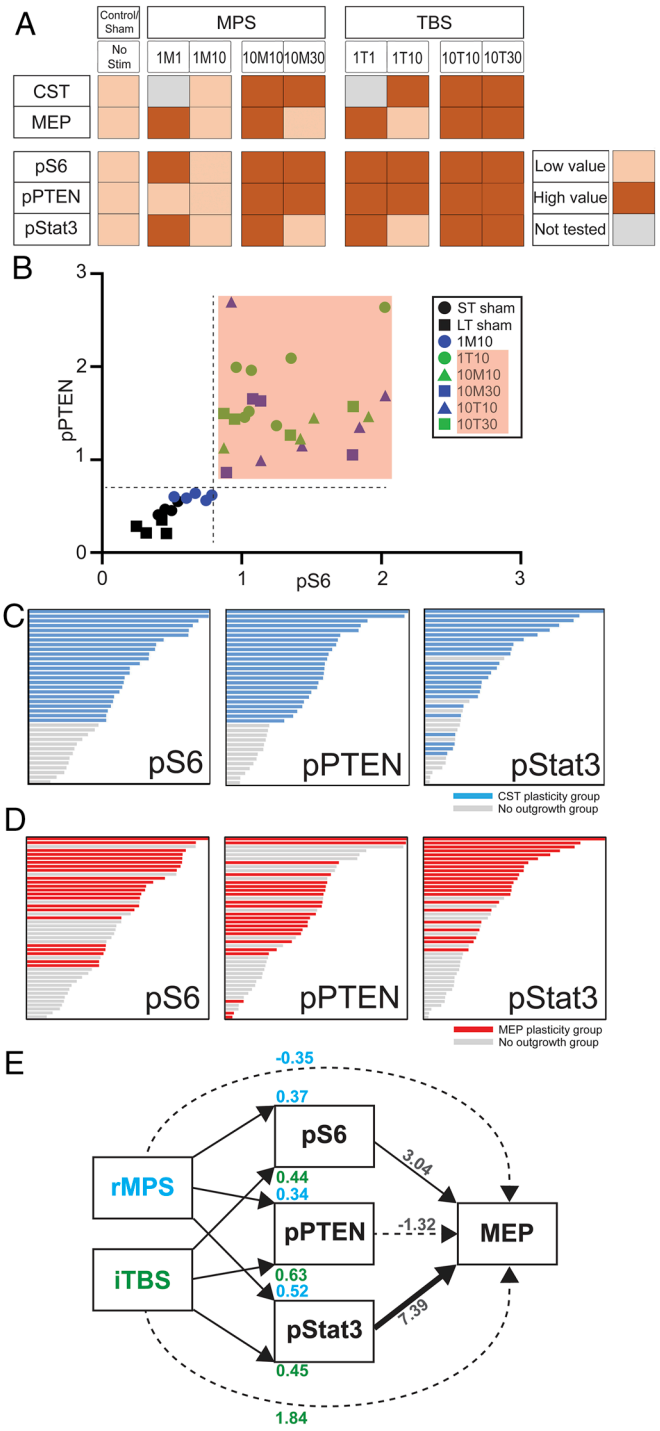

Fig. 7. Molecular marker analyses for CST sprouting and MEP enhancement. (*A*) Summary of CST and MEP enhancement results and their association with pS6, pPTEN, and pStat3 expression levels in the various experimental conditions. (*B*) Scatter plot of pS6 and pPTEN expression levels for CST assessment conditions. The red-highlighted quadrant represents experimental conditions in which significant CST outgrowth was identified. (*C*) Protein expression and CST sprouting. Graphs showing experimentally determined protein expression levels (bar length), rank-ordered. Blue bars indicate conditions where significant CST outgrowth was observed; gray bars, without significant CST outgrowth. Note pS6 and pPTEN, but not pStat3, thresholds for identifying CST plasticity groups. (*D*) Protein expression and MEP plasticity. Similar to part *C*, but for MEP plasticity. Red bars indicate conditions where significant MEP enhancement was observed; gray bars, without significant MEP enhancement. (*E*) MEP mediation analysis model showing effectiveness of MPS and iTBS in promoting MEP enhancement directly (curved dashed lines; both not significant) and in promoting significant MEP enhancement via pS6, pPTEN, and pStat3 expression, as mediators. The model also shows contributions of rMPS and iTBS in promoting significant molecular changes (*Left* side, solid lines). Solid lines indicate significant effects; dotted lines, lack of significance. Numerical values indicate b coefficients (*SI Appendix, Supplemental Material 2*).

PTEN and produced transient pS6 elevation; this did not result in CST growth. It is possible that sprouting could not be initiated due to insufficiencies in growth signaling. Evidence for such noncanonical activation of mTOR signaling independent of PTEN deactivation includes protein complexes, such as Tuberous Sclerosis Complex, upstream of mTOR and can activate mTOR signaling in response to neurotrophins without altering PTEN levels (27, 28). Since short-term MPS did not produce CST sprouting, we did not pursue the significance and mechanisms of potential noncanonical mTOR regulation further. Neurotrophin signaling has been shown for neuromodulation protocols that produce motor cortex plasticity and excitability changes (e.g., direct current stimulation), resulting in significant changes in brain-derived neurotrophic factor (BDNF/trkB signaling and diminished neuromodulation efficacy with expression of the BDNF val66Met polymorphism (29, 30). Additionally, numerous long noncoding RNAs and microRNAs have been documented that regulate mTOR signaling by directly interacting with mTORC1 (reviewed in ref. 31). Future experiments are needed to determine the role of BDNF/trkB signaling in neuromodulation efficacy, as well as other mechanisms, and their interactions with mTOR signaling. Short-term iTBS effectively phosphorylated PTEN and produced persistent pS6 elevation, resulting in significant CST outgrowth. Thus, the short-term protocols distinguished mTOR and PTEN changes, in a neuromodulation-dependent way. Both long-term rMPS and iTBS were associated with effective mTOR activation and PTEN deactivation and, in turn, CST growth. These findings are consistent with our earlier finding that the mTOR blocker rapamycin prevented CST sprouting when administered during the period of neuromodulation [rMPS;(16)].

Jak/Stat activation (pStat3) in retinal ganglion cells and CST neurons is associated with axon regeneration/outgrowth (32–35). This has been demonstrated after injury by persistent Stat3 activation (32) and deletion of its antagonist/repressor SOCS3 (33). Further, codeletion of PTEN with SOCS3 produces greater optic nerve and CST axon outgrowth than SOCS3 alone (34, 35). Using logistic regression, we show a statistically significant association between pStat3 protein levels and whether an animal was in a group that showed CST sprouting (10M10, 10T10, 10T30). Despite strong associations with axon growth, we found dissociation between pStat3 activation and CST outgrowth for two conditions (10M30; 1T10), suggesting that neuromodulation recruits additional mechanisms that are not dependent on Stat3 for producing outgrowth. One mechanism may be through supporting axon maintenance by activity-dependent synaptogenesis. Pharmacological blockade of Stat3 phosphorylation prevents CST activity-dependent synaptogenesis without affecting CST axon growth [by rMPS; (16)]. This is consistent with the present study that pStat3 is the principal mediator of MEP plasticity and with studies demonstrating a role for pStat3 in long-term synaptic plasticity (36). Neuromodulation may recruit mTOR-Jak/Stat interactions to support axon growth, as shown by our mediation assay, and suggested by the ability of SOCS3 deletion to restore injury-dependent loss of mTOR activity (33).

iTBS Activates Both mTOR and Jak/Stat Signaling after SCI. Bilateral SCI, which axotomizes most CST axons in the spinal cord (37), did not prevent expression of the molecular markers of CST growth (i.e., elevated mTOR signaling and pPTEN protein). This is consistent with our prior SCI study (14), which showed robust CST sprouting rostral to a cervical contusion injury with iTBS. In maturity, immunostaining of retrogradely identified axotomized CST neurons shows a decline in mTOR signaling after pyramidal tract lesion (18). By contrast, we found that pS6 baseline levels

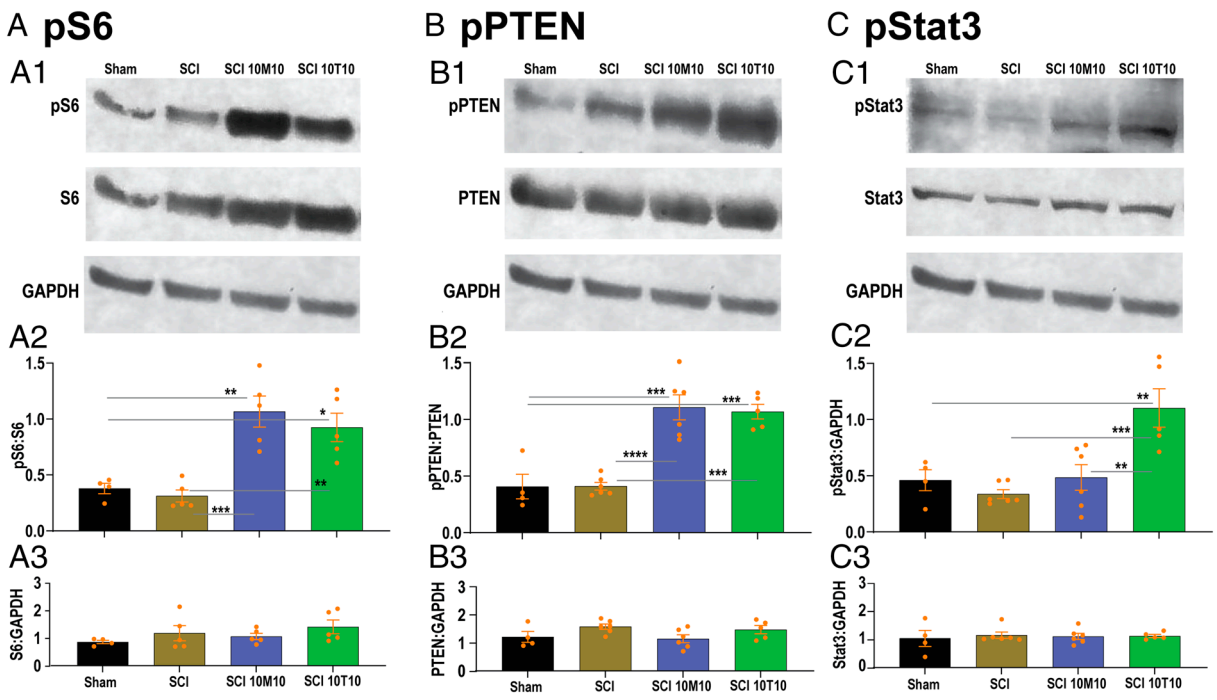

Fig. 8. Protein expression after SCI. (*A*) pS6 protein expression. (*A1*) Western blot images of cortical lysates probed with antisera against phospho-S6, total S6, and GAPDH. (*A2*) Mean intensities of pS6 expression, presented as ratios of pS6 to total S6. Asterisks denote significant difference $^{**}P = 0.0023$ (Sham vs. SCI 10M10); $^{*}P = 0.0141$ (Sham vs. SCI 10T10); $^{***}P = 0.0006$ (SCI vs. SCI 10M10); $^{**}P = 0.0037$ (SCI vs. SCI 10T10). One-way ANOVA with Tukey's multiple comparisons test. Sham group, n = 4; SCI, n = 5; SCI 10M10, n = 5; SCI 10T10, n = 5. (*A3*) Mean intensities of total S6 expression, presented as ratios of total S6 to GAPDH. One-way ANOVA with Tukey's multiple comparisons test shows no significant difference between groups. (*B*) pPTEN protein expression. (*B1*) Western blots probed with antisera against phospho-PTEN, total PTEN, and GAPDH. (*B2*) Mean intensities of pPTEN expression, presented as ratios of pPTEN to total PTEN. Asterisks denote significant difference $^{***}P = 0.0002$ (Sham vs. SCI 10M10); $^{****}P = 0.0004$ (Sham vs. SCI 10T10); $^{****}P = 0.0001$ (SCI vs. SCI 10M10); $^{***}P = 0.0001$ (SCI vs. SCI 10T10). One-way ANOVA with Tukey's multiple comparisons test. Sham, n = 4; SCI, n = 5; SCI 10M10, n = 6; SCI 10T10, n = 5. (*B3*) Mean intensities of total PTEN expression, presented as ratios of total PTEN to GAPDH. One-way ANOVA with Tukey's multiple comparisons test shows no significant difference between groups. (*C*) pStat3 protein expression. (*C1*) Western blot probed with antisera against phospho-Stat3, total Stat3, and GAPDH. (*C2*) Mean intensities of pStat3 expression, presented as ratios of pStat3 to total Stat3. Asterisks denote significant difference $^{**}P = 0.84$ (Sham vs. SCI 10M10); $^{***}P = 0.0007$ (SCI vs. SCI 10T10); $^{**}P = 0.005$ (SCI 10M10 vs. SCI 10T10). One-way ANOVA with Tukey's multiple comparisons test. Sham, n = 4; SCI, n = 5; SCI 10M10, n = 5; SCI 10T10, n = 5. (*C3*) Mean intensities of total Stat3 expression, presented as ratios of total Stat3 to GAPDH. One-way ANOVA with Tukey's multiple comparisons test shows no significant difference between groups.

and response to neuromodulation remained intact after cervical contusion injury, which axotomizes most CST axons in the spinal cord (37). Maintenance of baseline pS6 level may reflect preserved targeting of CST synapses to the rostral cervical spinal cord with a C4 SCI. The capacity for pS6 upregulation after neuromodulation is similar to induced mTOR upregulation in the pyramidal tract model with PTEN gene deletion (18). Whereas mTOR is activated in layer five pyramidal neurons with high-frequency stimulation in intact animals [e.g., pS6 upregulation; (16, 38)], activation of other cell classes that have not been axotomized by motor cortex neuromodulation, including glia, cannot be ruled out. Although both iTBS and rMPS were capable of activating mTOR signaling and deactivating PTEN protein after SCI, only iTBS was also capable of activating Jak/Stat. Intriguingly, this difference is not likely to be due to an activity "dose," as the number of simulation pulses delivered with rMPS is 50× greater than with iTBS (151,200 versus 3,000 stimulus pulses per session). Instead, it likely reflects differences in the temporal structure of the two protocols. This suggests that only iTBS can recruit both growth signaling and MEP plasticity after injury. This may have a beneficial impact on recovery.

Motor Cortex Neuromodulation Mimics Genetic Manipulation for Augmenting mTOR Signaling. That molecular signaling pathways can be harnessed through motor cortex neuromodulation in adult animals is significant for activity-dependent reshaping of corticospinal circuits after injury. Whereas limited lesion-dependent CST sprouting can occur in maturity after injury (12, 39), the capacity to produce significant CST axon growth in maturity has only been shown by genetic manipulations (17, 34, 40). For example, PTEN gene ablation produces CST axon growth through a spinal lesion (17) and substantially augments injury-dependent CST sprouting of the intact tract after unilateral pyramidotomy (41). Selective pharmacological suppression of PTEN in mice after dorsal hemisection stimulated growth of descending serotonergic fibers and limited CST growth in the caudal spinal cord (40). Our finding that motor cortex neuromodulation activates mTOR signaling and deactivates PTEN protein function, leading to CST sprouting, suggests that neuromodulation shares common mechanisms with genetic manipulation in promoting aspects of CST axon outgrowth. However, there is an important distinction. PTEN is a tumor-suppressor gene (reviewed in ref. 42), and can have negative consequences with ablation or inhibition, limiting clinical translation of PTEN gene manipulation in humans. Neuromodulation, on the other hand, can replicate aspects of growth-promoting signaling like genetic manipulation but without affecting PTEN gene expression or producing CST soma structural changes (16). Instead, neuromodulation promotes growth through posttranslational modification—a dynamic process that shifts the equilibrium between activated, nonphosphorylated, PTEN protein and its deactivated, phosphorylated, version. This is kinase dependent and reversible; it likely places the body at a lower risk of negative consequences.

Motor Cortex Neuromodulation Achieves Parallel Structural and Physiological Plasticity for Motor Recovery. MEP enhancement and CST outgrowth produced by motor cortex neuromodulation

are not necessarily causally linked. The presence of robust CST sprouting after short-term iTBS at day 10 is not associated with MEP enhancement. Whereas long-term protocols were effective in MEP enhancement, only iTBS was capable of producing persistent enhancement at the 30-d time point. Furthermore, we show that pStat3 elevation is the key mediator of MEP plasticity. Blockade of pStat3 phosphorylation during rMPS, which does not impair CST sprouting (16), is consistent with uncoupling of pStat3 activation and CST sprouting. A key question raised by these findings is under what circumstances neuromodulation recruits both mTOR and Jak/Stat signaling for sprouting and MEP plasticity? There is a potential interplay between structural and physiological plasticity that seems to be critical for achieving CST functional repair, which needs to be examined.

Repeated bouts of daily neuromodulation are capable of driving structural plasticity at 10 d, with persistent activation of mTOR signaling and deactivation of PTEN protein by phosphorylation. Activated axon terminals may become stronger and, whether in the spinal cord or through brainstem pathways (43), evoke larger MEPs. The lack of persistent MEP enhancement with rMPS (1M10, 10M30) may portend vulnerability to pruning of connections that are recently sprouted. Maintenance of Stat3 phosphorylation may prevent forgetting the "muscle memory" associated with the stronger connectivity produced by neuromodulation. Coexpression of differential molecular programs for axon growth and MEP plasticity suggest the presence of parallel neuromodulation-dependent mechanisms, and stress use of neuromodulation protocols optimized to ensure maintenance of physiological plasticity to support axon growth.

Biomarkers and Biological Targets for Activity-Dependent Functional Repair. Most neuromodulation strategies to promote function after injury target relevant anatomical structures and use stimulation intensities that favor activation of particular neuronal classes, such as large-diameter afferent fibers with spinal epidural stimulation, or cortical neuron dendrites with transcranial direct current stimulation. The intended outcome is increased neuronal excitability in the targeted anatomical structure, which is hypothesized to facilitate generation and transmission of stronger control signals after injury (44). However, a broad range of neural activity-dependent processes are, in principle, potential targets for activity-based neuromodulation.

We focused on activity-dependent CST axonal outgrowth and synaptogenesis as targets for neuromodulation in adult animal models, based on the potent effects that manipulating motor cortex activity has on establishment of CST connections during development (11). Those findings directed us to explore mTOR, PTEN, and Jak/Stat as targets for neuromodulation since the same pathways have been manipulated genetically to drive CST outgrowth after SCI (18, 45–47). Not surprisingly, the stimulation parameters for effective neuromodulation are bewilderingly complex. Complexity is compounded by a wide array of potential outcome measures that are technically challenging and time consuming to quantify. Signaling pathways or genetic expression changes can be assayed after a period of neuromodulation more efficiently than CST outgrowth and MEP plasticity or other morphological measures (26, 48). We were surprised to observe such clarity in pS6 and pPTEN levels predicting neuromodulation-dependent CST growth. The presence of absolute threshold values precluded using mediation analysis. The molecular underpinnings of MEP plasticity, although robust, are probabilistic and dependent on multiple factors, such as neurotransmitter regulatory mechanisms (36). Mediation analysis showed that the direct effects of rMPS and iTBS on MEP plasticity were not significant, indicating that the outcome (MEP response enhancement) is produced via the molecular mediators. The analysis shows pStat3 is the key marker for MEP plasticity. Whereas the absolute levels of the biochemical markers may not directly compare across studies, our finding shows a molecular prediction of system-level outcomes.

Materials and Method

Animals and General Surgical Protocols. All experiments were conducted in accordance with the NIH Guidelines for the Care and Use of Laboratory Animals. All animal protocols were approved by the City University of New York Advanced Science Research Center Institutional Animal Care and Use Committee (IACUC). Adult female Sprague Dawley rats (250 and 300 g) were housed under a 12-h light/dark cycle in the institutional vivarium and provided with unrestricted access to food and water. *SI Appendix*, Table S1 lists animal groups, numbers, stimulation type and duration, and poststimulation follow-up periods. Surgeries were performed under general anesthesia using isoflurane (3.5% for induction and 1.5% for maintenance in 0.9L/min oxygen). Buprenorphine (0.01 mg/kg) was administered after surgery to alleviate pain. Anesthesia levels, heart rate, respiration rate, and temperature were continuously monitored during surgery. Rats were kept on a heating pad to maintain body temperature at 37.5 °C during surgery, and postsurgery until ambulatory.

Anterograde CST Tracer Injection. Rats were anesthetized and placed in a stereotaxic frame. Following craniotomy to expose the forelimb area of the primary motor cortex, seven pressure injections (300 ηL/each) of biotinylated dextran amine (BDA; 10,000 MW; Molecular Probes; 10% in 0.1 M phosphate buffered saline were made at a depth of 1.5 mm each). Tracer injections were made in the following anteroposterior (AP) and mediolateral (ML) coordinates within the forelimb area of the motor cortex (49, 50) relative to bregma (with minor adjustments for the locations of blood vessels): AP 0.5 m, ML 2 mm; AP 0.5 mm, ML 2.8 mm; AP 0.5 mm, ML 3.9 mm; AP 1.5 mm, ML 3.5 mm; AP 1.5 mm, ML 2.5 mm; AP 2.0 mm, ML 2.5 mm; AP 2.2 mm, ML 3.5 mm. Tracer was injected using a micropump (WPI) at an injection rate of 3 ηL/s.

Motor Cortex Electrode Implantation. A stainless steel bipolar stimulating electrode (Plastics One) was placed on the dura over the forelimb motor cortex (12). The electrode wires were bent into an "L" shape with the bottom of the "L" deinsulated. We placed the angle of the L-shaped electrodes approximately 2 mm anterior and 3.5 mm lateral to bregma, with the exposed contact extending rostrally over the forelimb M1. The electrode was positioned so that the deinsulated portion contacted the dura. The electrode was covered with dental acrylic cement, which was secured using bone screws (Plastics One).

C4 Spinal Contusion Injury. A laminectomy was performed and a C4 200 kdyn midline contusion (14). was made using an Infinite Horizon spinal impactor. After surgery, animals were returned to a holding cage that was placed up a heating pad and observed until ambulatory. An antibiotic (Baytril; 5 mg/kg) was administered.

rMPS and iTBS. Electrical rMPS consisted of trains of repetitive stimuli (0.2 ms duration, 333 Hz, 45 ms bursts, every 2 s), delivered 6 h/d (12). Electrical iTBS consists of a burst of three pulses (interstimulus interval: 50 ms), repeated 10 times, for 2 s followed by 8 s without stimulation; this was repeated 20 times, for a total of 600 pulses (13). This single iTBS block was

repeated five times with 2 min between blocks, for a total time of approximately 30 min. Stimulus intensity for rMPS and iTBS was determined using brief pulse trains (330 Hz; 45 ms duration, 14 pulses). For rMPS, threshold current was adjusted to the minimal value needed to evoke a contralateral forelimb movement for approximately 50% of the stimuli presented, which was typically between 1 to 2 mA. At motor threshold, stimulation did not evoke an ipsilateral forelimb movement or movements of either hind limb. For iTBS, current intensity was chosen as 75% of motor threshold. In separate animal cohorts, rMPS and iTBS were administered for 1 d (short-term) or 10 d (long-term). Animals were awake during stimulation.

Western Blot Analyses. For western blotting, experiments were terminated (100 mg/kg Euthasol; Vedco, Missouri, USA) within 30 min after stimulation or after a predetermined delay period (Fig. 1 and *SI Appendix*, Table S1) and the brain was removed. The motor cortices were dissected and placed into ice-cold Hank's balanced salt solution (Invitrogen). The forelimb M1 region was placed in a microtube and homogenized promptly in neuronal protein extraction reagent buffer (Invitrogen), supplemented with a protease-inhibiting cocktail and ethylenediaminetetraacetic acid (Invitrogen). Bradford protein analysis was used to measure protein concentration; approximately 50 µg of protein was subjected to sodium dodecyl sulfate acrylamide-bisacrylamide gel electrophoreses along with a protein ladder (Crystalgen #65-0671) for size comparison. Following electrophoresis, the protein bands were transferred to polyvinylidene difluoride membrane (Millipore #IPVH08130) and probed against the primary antibodies (*SI Appendix*, Supplemental Material 3). An electrochemiluminescent system (Cell Signaling Technology #6883P3) was used to develop the western blots. It should be noted that in western blot experiments, pStat3 protein bands often appear as close doublets. These are splice variants alpha (top) and beta (bottom) isoforms (51). They are treated as a single band for densitometry analyses.

Tracer Histochemistry. Animals were deeply anesthetized with 100 mg/kg of Euthasol (Vedco, Missouri, USA) and transcardially perfused with saline, followed by 4% paraformaldehyde. Tissue was postfixed in 4% paraformaldehyde for 1 to 2 h and transferred to 20% sucrose (overnight at 4 °C). Frozen sections were cut transversely at 40 µm thickness using a sliding microtome. BDA was visualized with 1% avidin–biotin complex reagent (ABC kit; Vector Laboratories), followed by the chromogen diaminobenzidine (Sigma).

Contralateral Spinal CST Sprouting assay. Neurolucida (MBF Bioscience, Williston, VT) was used to measure axon length at 100× magnification with oil immersion in a region of interest in the contralateral intermediate zone (200 × 200 mm^2; 400 mm lateral to central canal) at spinal C7 and C8 levels. Axon lengths were measured in three to five transverse sections for each animal by laboratory personnel blinded to the animal group. To correct measurements for tracer efficacy, contralateral BDA-labeled CST axons within the dorsal column were counted at 100× magnification with oil immersion (Optical Fractionator counting protocol, Stereo Investigator software; MBF Bioscience, VT). For stereological counting, section thickness (cut at 40 µm) was estimated to be 35 µm after accounting for tissue shrinkage. The total axon length for each section was corrected for tracer efficacy by dividing measured axon length/average number of BDA-labeled CST axons in the dorsal column in three to five sections of the same animal (26).

MEP Enhancement. Electromyographic (EMG) recordings were conducted in sedated animals (ketamine, 70 mg/kg; xylazine, 10 mg/kg) in response to motor cortex simulation using the implanted epidural electrode, to produce MEPs (13). Wire electrodes were inserted percutaneously into the extensor carpi radialis muscle and recruitment curves were generated using triple biphasic pulses (0.2 ms) delivered every 3 s between threshold (1.0) and 1.6-times threshold current in random order. To compare results across assessments on different days, stimulation was performed in relation to threshold current value. Current thresholds (the lowest current that produced an EMG response in 50% of trials) were determined at the start of each session. EMGs were acquired with a differential AC amplifier system (A-M Systems), at a gain of 1,000 and bandpass filtered between 10-5K Hz. A commercial data acquisition system (Power 1401, SPIKE2 software; Cambridge Electronic Design Ltd.) was used at a sampling rate of 5,000 Hz. Raw EMG signals were rectified before processing. The AUC for the EMG was quantified between the onset and the end of the response (*SI Appendix*, Fig. S3). The value of baseline EMG, corresponding to the duration of the response measured over 100 ms before the first stimulus, was subtracted from the value of the evoked response. The EMG AUC was averaged based on a minimum of 25 frames (500 ms duration) per test to ensure accuracy and reliability of the measurements.

During initial pilot experiments, we observed that MEP thresholds were elevated immediately after chronic rMPS or iTBS and for up 3 d. To ensure stable current thresholds and evoked responses, we delayed performing MEP recruitment experiment for 3 d after the last rMPS or iTBS neuromodulation session. This period is indicated in the Results section as the acute poststimulation period.

Mediation Analysis. To assess the importance of proteins pS6, pPTEN, and pStat3 in achieving the plasticity outcomes—CST axon sprouting and MEP enhancement—we performed a model-based statistical analysis. The model (Fig. 7*E*) assumes that pS6, pPTEN, and pStat3 are each potential mediators of the effects of rMPS and iTBS as causes of the plasticity outcome, in addition to possible direct effects (i.e., direct action of rMPS and iTBS on outcomes, without mediation by any of the proteins). Mediation analysis consists of running two models: The first model captures the effect of the causes on the mediators, and the second model captures the effects of all variables on the outcome including direct effects (52). Therefore, we first estimated the effect of rMPS and iTBS on each of the three proteins using linear regression. For pStat3:

$$\mathrm{pSTAT3} \sim b_{1,\mathrm{rmps}} * \mathrm{rMPS} + b_{1,\mathrm{tbs}} * \mathrm{TBS} + b_{1,0}.$$

This was performed similarly for pS6 and pPTEN. Then we estimated the effect of pS6, pPTEN, and pStat3 on MEP, with iTBS and rMPS as control variables using logistic regression because the MEP outcome here were binary (MEPs were enhanced or not enhanced):

$$\mathrm{logit}(\mathrm{MEP}) \sim b_{2,\mathrm{PMS}} * \mathrm{rMPS} + b_{2,\mathrm{tiTBS}} * \mathrm{iTBS} + b_{2,\mathrm{pS6}} * \mathrm{pS6} + b_{2,\mathrm{pStat3}} * \mathrm{pStat3} + b_{2,\mathrm{pPTEN}} * \mathrm{pPTEN} + b_{2,0}.$$

We performed a similar analysis for CST outgrowth as binary outcomes (CST axon length was enhanced or not enhanced). Both linear and logistic regressions were implemented using the fitglm function in MATLAB with linear and logit link functions, respectively.

The parameters b_1 and b_2 of the linear and logistic regressions models, respectively, can be combined to determine the odds ratio of the outcomes. Odds ratio quantifies the odds that an outcome will occur (vs. not occur) given a particular treatment. For instance, an odds ratio of three for TBS onto MEP means that a treatment with TBS will increase the likelihood of observing an enhanced MEP by a factor of three (a 200% increase). The odds ratio can be computed from b_1 and b_2 as follows: the odds ratio of the direct effects is $\exp(b_2)$ and for the indirect effect they are $\exp(b_1{*}b_2)$, and the total effect on odds ratio is the product of both, $\exp(b_2{+}b_1{*}b_2)$ (*SI Appendix*, Table S2).

Statistics and General Data Analyses. All anatomical and EMG response measurements were performed by laboratory staff blinded to treatment condition. Statistical analyses were performed using Prism 8 (GraphPad Software), Excel (Microsoft), R (4.3.0 - 2023), and Matlab. The differences between experimental groups were determined using one of the following statistical tests: Mann–Whitney *t* test, one-way or two-way ANOVA with either Tukey's post hoc, Dunnett's or Sidak's multiple comparison tests and Fisher's exact test. We used the web-based calculator, powerandsamplesize.com, to conduct power analyses for the WB experiments.

Data, Materials, and Software Availability. Study data values were deposited at the Open Data Commons for Spinal Cord Injury (ODC-SCI; RRID:SCR_016673) (53). The ODC-SCI is a secure, cloud-based repository platform designed to share research data (54). All other data are included in the article and/or *SI Appendix*.

ACKNOWLEDGMENTS. We thank XiuLi Wu for histology and Dr. Sulli Popilskis and the staff of the City University of New York Advanced Science Research Center Vivarium for veterinary care. This work was supported by the NIH (J.H.M.: 2R01NS064004; L.C.P. and J.H.M. Multiple Principal Investigatorsl 1R01NS130484); New York State Department of Health Spinal Cord Injury Research Board (J.H.M.: C37716GG); and Craig H. Neilsen Foundation (N.Z.: CHN 385743).

Author affiliations: [a]Department of Molecular, Cellular, and Biomedical Sciences, Center for Discovery and Innovation, City University of New York School of Medicine, New York, NY 10031; [b]Department of Educational Psychology, Graduate Center of the City University of New York, New York, NY 10016; [c]Department of Biomedical Engineering, Grove School of Engineering, The City College of New York, New York, NY 10031; and [d]Neuroscience Program, Graduate Center of the City University of New York, New York, NY 10016

1. J. Long, P. Federico, M. A. Perez, A novel cortical target to enhance hand motor output in humans with spinal cord injury. *Brain* **140**, 1619–1632 (2017).
2. V. Di Lazzaro, J. C. Rothwell, Corticospinal activity evoked and modulated by non-invasive stimulation of the intact human motor cortex. *J. Physiol.* **592**, 4115–4128 (2014).
3. J. B. Carmel, J. H. Martin, Motor cortex electrical stimulation augments sprouting of the corticospinal tract and promotes recovery of motor function. *Front. Integr. Neurosci.* **8**, 51 (2014).
4. A. Pal *et al.*, Spinal cord associative plasticity improves forelimb sensorimotor function after cervical injury. *Brain* **145**, 4531–4544 (2022).
5. S. Moorjani, S. Walvekar, E. E. Fetz, S. I. Perlmutter, Movement-dependent electrical stimulation for volitional strengthening of cortical connections in behaving monkeys. *Proc. Natl. Acad. Sci. U.S.A.* **119**, e2116321119 (2022).
6. F. Maeda, J. P. Keenan, J. M. Tormos, H. Topka, A. Pascual-Leone, Modulation of corticospinal excitability by repetitive transcranial magnetic stimulation. *Clin. Neurophysiol.* **111**, 800–805 (2000).
7. M. A. Nitsche, W. Paulus, Excitability changes induced in the human motor cortex by weak transcranial direct current stimulation. *J. Physiol.* **527**, 633–639 (2000).
8. A. Amer, J. H. Martin, Repeated motor cortex theta-burst stimulation produces persistent strengthening of corticospinal motor output and durable spinal cord structural changes in the rat. *Brain. Stimul.* **15**, 1013–1022 (2022).
9. Y.-Z. Huang, M. J. Edwards, E. Rounis, K. P. Bhatia, J. C. Rothwell, Theta burst stimulation of the human motor cortex. *Neuron* **45**, 201–206 (2005).
10. A. Amer, J. Xia, M. Smith, J. H. Martin, Spinal cord representation of motor cortex plasticity reflects corticospinal tract LTP. *Proc. Natl. Acad. Sci. U.S.A.* **118**, e2113192118 (2021).
11. J. Martin, K. Friel, I. Salimi, S. Chakrabarty, "Corticospinal development" in *Encyclopedia of Neuroscience*, L. Squire Ed. (Academic Press, Oxford, 2009), pp. 302–314.
12. M. Brus-Ramer, J. B. Carmel, S. Chakrabarty, J. H. Martin, Electrical stimulation of spared corticospinal axons augments connections with ipsilateral spinal motor circuits after injury. *J. Neurosci.* **27**, 13793–13801 (2007).
13. W. Song, A. Amer, D. Ryan, J. H. Martin, Combined motor cortex and spinal cord neuromodulation promotes corticospinal system functional and structural plasticity and motor function after injury. *Exp. Neurol.* **277**, 46–57 (2016).
14. N. Zareen *et al.*, Motor cortex and spinal cord neuromodulation promote corticospinal tract axonal outgrowth and motor recovery after cervical contusion spinal cord injury. *Exp. Neurol.* **297**, 179–189 (2017).
15. J. H. Martin, B. Kably, A. Hacking, Activity-dependent development of cortical axon terminations in the spinal cord and brain stem. *Exp. Brain. Res.* **125**, 184–199 (1999).
16. N. Zareen *et al.*, Stimulation-dependent remodeling of the corticospinal tract requires reactivation of growth-promoting developmental signaling pathways. *Exp. Neurol.* **307**, 133–144 (2018).
17. K. K. Park *et al.*, Promoting axon regeneration in the adult CNS by modulation of the PTEN/mTOR pathway. *Science* **322**, 963–966 (2008).
18. K. Liu *et al.*, PTEN deletion enhances the regenerative ability of adult corticospinal neurons. *Nat. Neurosci.* **13**, 1075–1081 (2010).
19. A. Suppa *et al.*, Ten years of theta burst stimulation in humans: Established knowledge, unknowns and prospects. *Brain. Stimul.* **9**, 323–335 (2016).
20. J. Jaworski, M. Sheng, The growing role of mTOR in neuronal development and plasticity. *Mol. Neurobiol.* **34**, 205–219 (2006).
21. J. O. Lipton, M. Sahin, The neurology of mTOR. *Neuron* **84**, 275–291 (2014).
22. F. Vazquez, W. R. Sellers, The PTEN tumor suppressor protein: An antagonist of phosphoinositide 3-kinase signaling. *Biochim. Biophys. Acta* **1470**, M21–M35 (2000).
23. J. Torres, R. Pulido, The tumor suppressor PTEN is phosphorylated by the protein kinase CK2 at its C terminus. Implications for PTEN stability to proteasome-mediated degradation. *J. Biol. Chem.* **276**, 993–998 (2001).
24. A. M. Planas, M. Berruezo, C. Justicia, S. Barron, I. Ferrer, Stat3 is present in the developing and adult rat cerebellum and participates in the formation of transcription complexes binding DNA at the sis-inducible element. *J. Neurochem.* **68**, 1345–1351 (1997).
25. J. B. Carmel, H. Kimura, J. H. Martin, Electrical stimulation of motor cortex in the uninjured hemisphere after chronic unilateral injury promotes recovery of skilled locomotion through ipsilateral control. *J. Neurosci.* **34**, 462–466 (2014).
26. J. B. Carmel, L. J. Berrol, M. Brus-Ramer, J. H. Martin, Chronic electrical stimulation of the intact corticospinal system after unilateral injury restores skilled locomotor control and promotes spinal axon outgrowth. *J. Neurosci.* **30**, 10918–10926 (2010).
27. K. Inoki, Y. Li, T. Zhu, J. Wu, K. L. Guan, TSC2 is phosphorylated and inhibited by Akt and suppresses mTOR signalling. *Nat. Cell. Biol.* **4**, 648–657 (2002).
28. V. Briz *et al.*, Calpain-2-mediated PTEN degradation contributes to BDNF-induced stimulation of dendritic protein synthesis. *J. Neurosci.* **33**, 4317–4328 (2013).
29. B. Fritsch *et al.*, Direct current stimulation promotes BDNF-dependent synaptic plasticity: Potential implications for motor learning. *Neuron* **66**, 198–204 (2010).
30. B. Cheeran *et al.*, A common polymorphism in the brain-derived neurotrophic factor gene (BDNF) modulates human cortical plasticity and the response to rTMS. *J. Physiol.* **586**, 5717–5725 (2008).
31. K. Aboudehen, Regulation of mTOR signaling by long non-coding RNA. *Biochim. Biophys. Acta Gene. Regul. Mech.* **1863**, 194449 (2020).
32. C. Lang, P. M. Bradley, A. Jacobi, M. Kerschensteiner, F. M. Bareyre, STAT3 promotes corticospinal remodelling and functional recovery after spinal cord injury. *EMBO Rep.* **14**, 931–937 (2013).
33. P. D. Smith *et al.*, SOCS3 deletion promotes optic nerve regeneration in vivo. *Neuron* **64**, 617–623 (2009).
34. F. Sun *et al.*, Sustained axon regeneration induced by co-deletion of PTEN and SOCS3. *Nature* **480**, 372–375 (2011).
35. D. Jin *et al.*, Restoration of skilled locomotion by sprouting corticospinal axons induced by co-deletion of PTEN and SOCS3. *Nat. Commun.* **6**, 8074 (2015).
36. G. S. Mahmoud, L. M. Grover, Growth hormone enhances excitatory synaptic transmission in area CA1 of rat hippocampus. *J. Neurophysiol.* **95**, 2962–2974 (2006).
37. K. D. Anderson, K. G. Sharp, O. Steward, Bilateral cervical contusion spinal cord injury in rats. *Exp. Neurol.* **220**, 9–22 (2009).
38. M. Fujiki, K. M. Yee, O. Steward, Non-invasive high frequency repetitive transcranial magnetic stimulation (hfrTMS) robustly activates molecular pathways implicated in neuronal growth and synaptic plasticity in select populations of neurons. *Front. Neurosci.* **14**, 558 (2020).
39. M. Thallmair *et al.*, Neurite growth inhibitors restrict plasticity and functional recovery following corticospinal tract lesions. *Nat. Neurosci.* **1**, 124–131 (1998).
40. Y. Ohtake, U. Hayat, S. Li, PTEN inhibition and axon regeneration and neural repair. *Neural Regen. Res.* **10**, 1363–1368 (2015).
41. D. H. Lee *et al.*, Mammalian target of rapamycin's distinct roles and effectiveness in promoting compensatory axonal sprouting in the injured CNS. *J. Neurosci.* **34**, 15347–15355 (2014).
42. X. Liu, P. R. Williams, Z. He, SOCS3: A common target for neuronal protection and axon regeneration after spinal cord injury. *Exp. Neurol.* **263**, 364–367 (2015).
43. J. B. Carmel, H. Kimura, L. J. Berrol, J. H. Martin, Motor cortex electrical stimulation promotes axon outgrowth to brain stem and spinal targets that control the forelimb impaired by unilateral corticospinal injury. *Eur. J. Neurosci.* **37**, 1090–1102 (2013).
44. M. Oudega, M. A. Perez, Corticospinal reorganization after spinal cord injury. *J. Physiol.* **590**, 3647–3663 (2012).
45. K. Zukor *et al.*, Short hairpin RNA against PTEN enhances regenerative growth of corticospinal tract axons after spinal cord injury. *J. Neurosci.* **33**, 15350–15361 (2013).
46. G. Lewandowski, O. Steward, AAVshRNA-mediated suppression of PTEN in adult rats in combination with salmon fibrin administration enables regenerative growth of corticospinal axons and enhances recovery of voluntary motor function after cervical spinal cord injury. *J. Neurosci.* **34**, 9951–9962 (2014).
47. C. A. Danilov, O. Steward, Conditional genetic deletion of PTEN after a spinal cord injury enhances regenerative growth of CST axons and motor function recovery in mice. *Exp. Neurol.* **266**, 147–160 (2015).
48. B. R. Kondiles, R. L. Murphy, A. J. Widman, S. I. Perlmutter, P. J. Horner, Cortical stimulation leads to shortened myelin sheaths and increased axonal branching in spared axons after cervical spinal cord injury. *Glia* **71**, 1947–1959 (2023).
49. M. Brus-Ramer, J. B. Carmel, J. H. Martin, Motor cortex bilateral motor representation depends on subcortical and interhemispheric interactions. *J. Neurosci.* **29**, 6196–6206 (2009).

50. E. J. Neafsey *et al.*, The organization of the rat motor cortex: A microstimulation mapping study. *Brain Res.* **396**, 77–96 (1986).
51. D. Maritano *et al.*, The STAT3 isoforms alpha and beta have unique and specific functions. *Nat. Immunol.* **5**, 401–409 (2004).
52. T. VanderWeele, *Explanation in Causal Inference: Methods for Mediation and Interaction* (Oxford University Press, United Kingdom, 2015).
53. N. Zareen *et al.*, Motor cortex neuromodulation activates molecular signaling necessary for corticospinal axon growth and muscle response plasticity in intact rats and in rats with bilateral cervical spinal cord injury. Open Data Commons for Spinal Cord Injury. https://doi.org/10.34945/F5BG6S. Deposited 31 October 2024.
54. A. Torres-Espin *et al.*, Promoting FAIR data through community-driven agile design: The open data commons for spinal cord injury (odc-sci.org). *Neuroinformatics* 20, 203–219 (2022).